Limitation of the long-lived Te-121 contaminant in production of I-123 through the Xe-124(p,x) route

ARTICLE *in* APPLIED RADIATION AND ISOTOPES: INCLUDING DATA, INSTRUMENTATION AND METHODS FOR USE IN AGRICULTURE, INDUSTRY AND MEDICINE · FEBRUARY 2011

Impact Factor: 1.23 · DOI: 10.1016/j.apradiso.2010.10.013 · Source: PubMed

Applied Radiation and Isotopes 69 (2011) 358–368

Contents lists available at ScienceDirect

Applied Radiation and Isotopes

journal homepage: www.elsevier.com/locate/apradiso

Limitation of the long-lived ^{121}Te contaminant in production of ^{123}I through the ^{124}Xe(p,x) route

A. Hermanne [a,*], F. Tarkanyi [b], S. Takacs [b], R. Adam Rebeles [a], A. Ignatyuk [c], S. Spellerberg [d], R. Schweikert [e]

[a] Vrije Universiteit Brussel (VUB), 1090 Brussels, Belgium
[b] Institute of Nuclear Research of the Hungarian Academy of Sciences (ATOMKI), 4026 Debrecen, Bem ter 18/c, Hungary
[c] Institute of Physics and Power Engineering (IPPE), Obninsk 249020, Russia
[d] Institut ur Nuklearchemie, FZ Julich, Julich, Germany
[e] Zyklotron AG, Eggenstein-Leopoldshafen, Germany

ARTICLE INFO

Article history:
Received 6 March 2010
Accepted 20 October 2010

Keywords:
^{123}I production
^{121}I –^{121}Te contamination
^{122}Xe and $^{120m,g;119}$I isotopes
^{124}Xe gas cells
Cross sections
Nuclear model calculations

ABSTRACT

The 13.2 h half-life radioisotope ^{123}I is widely used in clinical nuclear medicine diagnosis. At present it is mostly produced in nca form by proton irradiation of highly enriched ^{124}Xe in dedicated gas target set-ups and relying on the decay chain ^{123}Cs–^{123}Xe–^{123}I.

Depending on the irradiation conditions contamination with long-lived ^{121}Te, a daughter product of the co-produced rather short lived ^{121}I, occurs and can limit the useful shelf life of the ^{123}I solution. Excitation function of the ^{124}Xe(p,α)^{121}I, ^{124}Xe(p,2n)^{123}Cs and ^{124}Xe(p,2p)^{123}Xe reactions are measured up to 35 MeV using the stacked gas cell technique and high-resolution γ-ray spectrometry. The experimental data were compared with the earlier literature values, with new results of the ALICE-IPPE and EMPIRE-II codes and with the data taken from the TENDL-2009 database. Existing discrepancies in cross-section data are largely solved and new recommended values are proposed. From fits to the new excitation curves integral ^{123}I batch yields and ^{121}Te contaminations for realistic production conditions are derived. Optimization of irradiation and cooling times and energy degradation in the target can strongly influence the contamination level.

1. Introduction

Due to its attractive radio-physical characteristics ^{123}I ($T_{1/2}$=13.2 h, decay for 100% by EC and emission of a 159 keV γ-line with abundance 83%) has gained a primordial role in SPECT nuclear medicine imaging. The longer shelf life and the lower costs of instrumentation compared to PET imaging have increased the market and clinical possibilities and at present it is used nearly worldwide. The large range of pharmaceuticals that can be labeled with iodine radionuclides allows a wide variety of applications from pharmacokinetics over functional imaging (fatty acids for myocardial cells metabolism, hippuric acid for renal studies, MIBG for tumors and heart studies) to recently receptor and transporter imaging.

At present the preferred route for ^{123}I production is bombardment of highly enriched ^{124}Xe gas with medium energy protons and taking advantage of the activation of the different radionuclides in the decay chain ^{123}Cs–^{123}Xe–^{123}I. After irradiation the gas targets are allowed to cool for several hours ensuring optimal in-growth of ^{123}I from its precursors. Separation of I, recovered from the walls of the irradiation cells, from all other elements, especially the stable ^{124}Xe target gas and residual ^{123}Xe, is performed resulting in an nca, pure solution. (Coenen et al., 2006; Tarkanyi et al., 1991a; Oberdorfer et al., 2009).

As the cross-section maxima for the reactions involved occur around 25 MeV(Tarkanyi et al., 1991a; Kurenkov et al., 1989), irradiations are performed with 30–35 MeV incident beams to ensure important yields. It has to be noted that although for the ^{124}Xe(p,2n)^{123}Cs reaction recommended cross-section values have been published in the IAEA TECDOC 1211 (IAEA, 2001) no such data were made available for the ^{124}Xe(p,pn)^{123}Xe reaction due to the large discrepancy existing between the two experimental data sets.

An unavoidable contaminant is ^{121}I ($T_{1/2}$=2.12 h) produced by the ^{124}Xe(p,α) reaction with a cross-section maximum around 20 MeV. This rather short lived radio-iodine will disappear quickly from the ^{123}I solution, but its long-lived decay product ^{121g}Te (16.8 d) accumulates and impairs the late use (several half-lives of ^{123}I after calibration date) of the solution.

Private information on practical production runs (Schweikert, Zyklotron AG) shows that in what is considered practical irradiation conditions (incident energy 35 MeV, degradation in the target to 20 MeV, irradiation time 13 h) the minimal ^{121}I – ^{121}Te level is reached at 12 after EOB and amounts to 3×10^{-3} of the ^{123}I activity.

No specific allowed ^{121}Te contamination limits are available in the European Pharmacopoeia where only a minimal purity of 99.7% ^{123}I is required. In an "Investigational Brochure" for High Specific Activity ^{123}I-MIBG (Mallinckrodt Medical BV) we found that the

* Corresponding author.
E-mail address: aherman@vub.ac.be (A. Hermanne).

0969-8043/$ - see front matter © 2010 Elsevier Ltd. All rights reserved.
doi:10.1016/j.apradiso.2010.10.013

producer specifies that at expiration date (=activity reference time+20 h) the ^{121}Te contamination level should be <900 Bq per MBq of ^{123}I or less than 9×10^{-4}. In a similar "Data sheet/directions for use; MIBG(^{123}I) injection " a limit of $<5\times10^{-4}$ is specified.

Further optimization, allowing a longer use of the solution after the reference time, could be obtained by lowering the ^{121}I production by limiting the target thickness and imposing higher exit energy or increasing the in-growth time beyond the optimal by allowing more decay of ^{121}I. Overall batch yield of ^{123}I will however also be influenced by these change in production parameters.

As the only experimental values for the ^{124}Xe(p,α)^{121}I reaction were reported in Tarkanyi et al. (1991b) and are limited to energies above 35 MeV, reliable data on the excitation function need to be measured for the first time in the energy region between threshold and 35 MeV.

Highly enriched ^{124}Xe in custom-made gas cells were bombarded with protons between 13 and 37 MeV with the double aim of determining cross sections for ^{121}I production and resolving discrepancies existing in the last published and evaluated values for production of ^{123}Cs and ^{123}Xe (direct and cumulative) (IAEA, 2001).

Also excitation curves for the minor, short lived co-produced radioisotopes ^{122}Xe and ^{119,120m,g}I are determined.

From fits to the newly obtained excitation curves, integral yields for different production circumstances are calculated. Given the half-lives of ^{123}Cs and ^{123}Xe on one side and of the ^{123}I on the other side it is well known that for short irradiations, or when only ^{123}Xe-containing gas would be removed from the target cell and transferred to a decay vessel where later the ^{123}I is recovered as proposed by Venikov et al. (1991), the optimal in growth time (yielding maximal ^{123}I activity) is 6.6 h. In commercial productions facilities however, irradiations lasting up to 20 h are performed and large amounts of ^{123}I activity, resulting from the decay of ^{123}Cs–^{123}Xe during the irradiation, are present in the irradiation cell. Hence additional contribution of ^{123}I in-growth after EOB is not so important anymore and possible cooling times before chemical processing (separation for recovery of the enriched ^{124}Xe target gas) are to be determined in function of decay of contaminants. We hence developed a calculation sheet allowing variation of incident energy, target thickness, irradiation time, cooling time and time of use of the ^{123}I solution makes it possible to optimize the different parameters in function of ^{123}I yield and minimization of ^{121}I content.

Also yields for short irradiations and fixed decay—in growth time (optimal is 6.6 h) can be calculated and are compared to the early experimental measurements as determined by Firouzbakht et al. (1987); Firouzbakht et al. (1992); Konyahin et al. (1989) and Iljin et al. (1987)

It has to be mentioned that in the less used alternative method discussed by Venikov, where only the activated target gas is transferred to a decay chamber, all radio-iodine formed during irradiation is discarded and hence no contamination with ^{121}I, or its decay product ^{121}Te, is present in the final ^{123}I solution (Venikov et al., 1991)

The experimentally determined cross sections are also compared with the results from different theoretical codes (ALICE-IPPE, EMPIRE II, latest version of TENDL database constructed from TALYS code).

2. Experimental techniques

2.1. Targets and irradiation

The excitation functions were measured by the activation technique using specially designed gas cells. Although the general technique is similar to what is described in Tárkányi et al. (2009) and references here in, some important differences in the set-up exist.

The stainless steel cells are truncated cones of length 25 mm with respective diameters of the entrance and exit ports of 10 and 25 mm. The change in geometry is introduced because, in comparison with cylindrical cells, the slanted surface of the side wall allow γ-rays emitted by the activated products adhering to the cell surface to reach the detector with no or strongly reduced absorption in the wall material

Gas tight closure is obtained by 2 Al windows of 52 μm thickness. Up to 5 of these cells can be attached to a filling station with connections for a vacuum pumping unit, pressure measurement, gas inlet and cryogenically recovery of irradiated gas.

After evacuation the cells were filled with highly enriched ^{124}Xe gas ($>99.92\%$ of Xe present, all other Xe isotopes $<0.01\%$) at absolute pressure between 0.28 and 0.86 bar.

The cells were irradiated at the external beam line of the CGR 560 cyclotron of Vrije Universiteit Brussel with proton beams of 150 nA intensity at 37.5, 29, 22.4, 16 and 13 MeV primary energies, obtained by changing the accelerator settings. The beam intensity was kept constant ($\pm10\%$) during the irradiations.

In each run one or at most 2 cells were placed in a closed cylindrical metal holder which served as a Faraday-cup for the initial beam current measurement.

In front and at the back of each cell 12.05- or 25-μm-thick Ti foils (depending on the experiment) were attached to monitor the beam intensity and to have additional information about effective incident particle energy.

Modification of this effective bombarding energy allowing to distribute evenly the measured cross section data points in the energy range studied is obtained by insertion of, as needed, one or several Al (52 and 156.5 μm) and Ta (210 μm) degrader foils in front of each cell.

According to our previous optical studies on the behavior of beam penetration in gas cells, no measurable density reduction along the beam path is observed at the low beam fluxes used. (Tarkanyi et al., 1997).

2.2. Post-irradiation handling and measurement

At the end of the bombardment the irradiated gas cells were first allowed to cool for a couple of minutes (decay of all very short lived contaminants formed in the target gas as ^{124m,g}Cs, ^{123m}Cs, ^{122g}Cs and short lived activation products in the monitor or degrader foils and the body of the cell). Afterwards the closed cells are placed in an ice-water bath at 0 °C for 5 min to allow settling of the produced Cs and I isotopes onto the wall of the chamber before starting the measurements. As all Cs, Xe and I radionuclides of interest have at least one independent γ-line of sufficient abundance (see Table 1), the activity and decay or in-growth over time can be followed by repeated short (5 min) assessment on a HPGe gamma-ray spectroscopy set-up for up to 1 or 2 h after EOB. Sample detector distance was adapted in function of the activity present and to assure that dead time was always below 10%. Efficiency calibration at the different distances was performed using standard reference sources.

2.3. Chemical recovery of radio-I

At the end of this measurement cycle the enriched ^{124}Xe gas (and remaining ^{123,122}Xe) was cryogenically recovered using the manifold described above.

To follow the formation of ^{121}Te through decay of ^{121}I a procedure was set up to recover quantitatively the I radionuclides

Table 1
Decay data of studied activation products and Q-values of contributing reactions.

Nuclide	$T_{1/2}$	$E\gamma$ (keV)	I_γ	Reaction	Q-value (MeV)
^{123}Cs	5.88 m	97.00	0.227	^{124}Xe(p,2n)^{123}Cs	−15.47
		596.60	0.101		
		741.50	0.030		
^{122}Xe	20.1 h	350.10	0.078	^{124}Xe(p,p2n)^{122}Xe	−18.5
		416.60	0.019	decay of ^{122}Cs by (p,3n)	−26.5
^{123}Xe	2.08 h	148.90	0.489	^{124}Xe(p,pn)^{123}Xe	−10.48
		178.00	0.149	decay of ^{123}Cs	
		330.00	0.086		
		899.60	0.024		
^{119}I	19.1 m	257.00	0.867	^{124}Xe(p,α2n)^{119}I	−15
				^{124}Xe(p,2p4n)^{119}I	−42
^{120g}I	1.35 h	560.00	0.696	^{124}Xe(p,αn)^{120g}I	−35.37
		641.00	0.084	^{124}Xe(p,αn)^{120m}I	−7.07
		1523.00	0.109	no decay from ^{120m}I	
^{120m}I	53 m	601.10	0.870	^{124}Xe(p,2p3n)^{120m}I	−35.37+(−0.32)
		614.00	0.671	^{124}Xe(p,αn)^{120m}I	−07.07+(−0.32)
		1345.90	0.190	no decay from ^{120}Xe	
		560.00	1.000		
^{121}I	2.12 h	212.20	0.843	^{124}Xe(p,2p2n)^{121}I	−24.8
				^{124}Xe(p,α)^{121}I	3.8
^{123}I	13.2 h	158.90	0.833	^{124}Xe(p,2p)^{123}I	−7
		528.90	0.014		
^{121}Te	19.16 d	507.60	0.177	^{124}Xe(p,3pn)^{121}Te	−21.76
		573.10	0.803		

formed during irradiation and decay. Unfortunately this did not allow to evaluate the total cumulative production of ^{123}I as not all ^{123}Xe had decayed to ^{123}I yet (chemistry is performed at less than $2T_{1/2}$ of ^{123}Xe after EOB). Only 6 out of the 15 cells were treated in this way.

Upon removal of the enriched ^{124}Xe cryogenically, the cells were filled through the gas filling inlet with a weak solution of NaI/$NaHSO_3$/HNO_3. Thereafter, the cells were vigorously shaken to ensure most of the radio-iodine that adhered on the cells wall was recovered. Next, one of the two Al windows of the cell was removed and the rinsing solution was carefully collected in a 100 ml beaker. The cell was than thoroughly rinsed with about 10 ml NaI/$NaHSO_3$/HNO_3 and the solution was collected in the same 100 ml beaker.

The iodine was precipitated by adding a small volume (5 ml) of 2% $AgNO_3$ solution and afterwards the precipitate was filtrated by means of a Millipore HVLP filter (20 mm diameter, 45 μm pore size). As the precipitation was not sufficient, 1 ml of 2% $AgNO_3$ was added to the filtrate and the solution was passed again through the same filter in order to ensure a higher cumulated yield.

After superficial drying, the filter with the precipitate is encapsulated in a home-made sample holder and covered with very thin polyethylene film. The mass of the precipitate was found to be around 0.0151 g after complete drying.

The efficiency of the procedure was checked by measuring the ^{123}I activity after each step and was found to be around 60%. This may be due to the possible losses of iodine during washing of the cells, transfer of the solution from the beaker to the filtration unit and a small amount of precipitate that adhered on the glass walls.

Measurements of the deposited samples were repeated several times over 25–30 days to follow the decay curve of ^{121}Te after total decay of ^{121}I. These measurements are not in good correlation with what can be derived from the ^{121}I activity present in the cells and are not discussed further here.

What about ^{123}I assessment after the chemical procedure? The precipitate contains only the *I that was formed directly or through decay of *Xe during the irradiation and the rather short cooling and measuring period. Possible further ^{123}I in-growth contributions are not possible as the remaining mother ^{123}Xe was removed together with the enriched Xe target gas. Time series measurements of the precipitate and applying a rather complex correction algorithm allows in principle to estimate the independent (p,2p) cross sections. As only a few data points are available, the uncertainties would be very high and as the low experimentally determined cross sections (Tarkanyi et al., 1989) are now confirmed by the new TALYS-2009 calculations (see Fig. 3b, value is 10 mb at 35 MeV) we did not attempt evaluation of the (p,2p) excitation function in this experiment.

2.4. Data processing

To determine the cross sections of reactions leading to the radioisotopes of interest only reactions on ^{124}Xe were taken into account. Other possible target isotopes do not contribute because of the high chemical purity of the target (> 99.9% Xe) and the high isotopic enrichment of ^{124}Xe (more than 99.6%). The amount of the stable ^{126}Xe isotope, the only that in the energy range considered could lead to the investigated radionuclides, is too small to be of any practical importance.

The evaluation of the gamma-ray peaks was made by the peak fitting algorithm provided with the GENIE analysis software.

The cross sections are calculated from the measured activities and irradiation parameters by using the activation and decay formulas. The nuclear decay characteristics of the radioisotopes studied are collected in Table 1 and were taken from the online NuDat database (Kinsey, 1997).

The beam intensity was estimated from the Faraday-cup measurement and corrected on the basis of the re-measured cross sections of activation in the monitor foils. The incident beam energy was initially derived from the accelerator settings calibrated by the time of flight method (Sonck et al., 1996) while the median energy in the cell, taken into account degradation in the Al and Ta foils and the gas at the actual filling pressure was

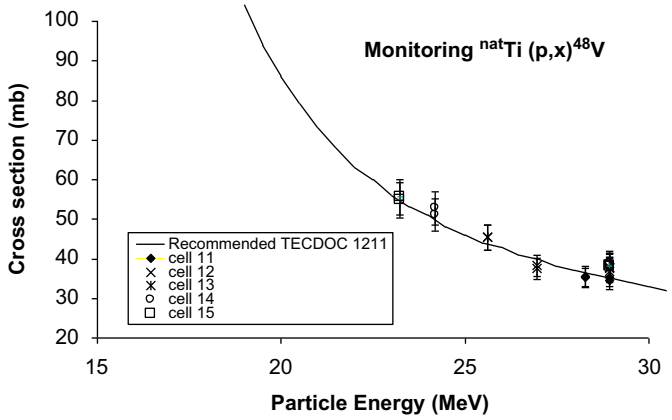

Fig. 1. Example of monitoring results for cells irradiated at primary energies of 29 MeV.

determined by a polynomial approximation of the stopping power (Andersen and Ziegler, 1977) The incident energy was corrected on the basis of the results of the activation of the monitor foils by the method described in Tárkányi et al. (1991c). An example of the monitoring results for the cells irradiated at primary energies of 29 MeV is shown in Fig. 1.

Standard data for the ^{nat}Ti(p,x)^{48}V monitor reaction were taken from (IAEA, 2001; Takacs et al., 2002).

The uncertainties on the directly calculated cross sections were estimated in the standard way as the square root of the quadratic sum of the independent relative uncertainties of the linearly contributing processes (ISO Guide, 1993). The individual contributions are: number of target nuclei (5%), particle flux (5%), decay parameters (2%), detection efficiency (2–5%) and statistical uncertainty on number of counts (1–5%).

For estimation of the uncertainty of the particle mean energy in the gas cells and in the monitor foils the cumulative errors influencing the calculated energy (incident proton energy, non-homogeneity and thickness variation of the foils and target gas, beam straggling) were taken into account.

The total cross section uncertainty amounts to 13% while the energy uncertainty varies between 0.2 and 0.7 MeV depending on the number and thickness of degrader foils.

3. Theoretical calculations

The excitation functions of the investigated reactions were evaluated by means of the statistical model codes ALICE-IPPE (Dityuk et al., 1998) and EMPIRE-II (Herman et al., 2007). A priori calculations were performed using the standard input parameter sets taken from RIPL-2 (Belgya et al., 2006) without any optimization to the target material or the reaction. Experimental data were also compared with the results of the TALYS-based Evaluated Nuclear Data Library TENDL-2009 (Koning and Rochman, 2009). The TALYS code performs model calculations in a way similar to the EMPIRE II, but uses a different selection of input parameters especially for the level densities and the optical potentials.

It should be noted that the ALICE code is based on a simplified version of the statistical model that do not take into consideration the low-lying discrete levels of residual nuclei. As a consequence, the EMPIRE II and TALYS results could be preferred as more accurate for the near threshold regions of various excitation functions. On the other hand, the pre-equilibrium model parameters in ALICE-IPPE are better adjusted to the high energy parts of charged-particle production cross sections and the ALICE-IPPE results could be preferable at high energies.

It is obvious that a much better description of experimental data for the most cases could be achieved with any statistical code after some adjustment of the model parameters. However for the present publication of new experimental data we restricted ourselves to calculations for the default input parameters (Belgya et al., 2006).

4. Results and discussion of excitation functions

4.1. Production of ^{123}I

As stated above the production of ^{123}I from proton induced reactions on ^{124}Xe is the result of three contributions: ^{124}Xe(p,2n) ^{123}Cs→^{123}Xe→^{123}I; ^{124}Xe(p,pn)^{123}Xe→^{123}I and ^{124}Xe(p,2p)^{123}I

As the half-life of ^{123}Cs is so short in any case measurement of the ^{123}Xe activity will always contain large contributions from the decay of the mother product during the irradiation, waiting and even measuring time. Hence assessment of the cross section of the (p,pn) reaction can best be done by subtracting the values for the (p,2n) reaction from the cumulative data for ^{123}Xe, measured after total decay of the parent ^{123}Cs.

4.1.1. ^{123}Cs excitation function

This short lived ($T_{1/2}$=5.9 min) primordial parent is measurable in the first half hour after EOB and can be assessed through 3 γ-lines at 97, 596 and 741 keV, respectively. Although the 97 keV line has the largest abundance it suffers from the relatively large uncertainty in determination of the detection efficiency at this energy near the maximum of the efficiency curve. The cross-sectional values are represented in Fig. 2a and indicated in Table 2a are based on the results at 596 keV averaged over the first 4 measurements. They correspond well to the calculated threshold and expected position of the maximum value for the ^{124}Xe(p,2n) reaction. Our new values are in good correspondence with the measured values of Tarkanyi et al. (1991a) and Kurenkov et al. (1989) and hence also with the recommended values of the TECDOC 1211 (IAEA, 2001) obtained to fit these literature data. It is to be remarked that these two literature sets have to be corrected by a constant factor due to the change in recent years for the adopted abundance used for the γ-line (at present in NuDat: 10.01%; earlier: 8.3% (Browne and Firestone, 1986) used in Tarkanyi et al. (1991a). No corrections for cross-sections data for the monitor reactions are needed as the reference values used in these articles are within a few percent of the present recommended values.

In Fig. 2a it can be seen that the maximum of the third-order polynomial fit to our data reaches a value of 520 mb at 24.8 MeV and occurs at a slightly lower energy and is about 5% higher than the corrected TECDOC-1211 (IAEA, 2001) value.

The predictions resulting from the different theoretical codes give widely scattered agreement with the new experimental points. The calculations with the ALICE-HMS (Blann, 1996) and ALICE-IPPE code already present in the TECDOC-1211 largely overestimated the values and showed energy shifts. The HF calculation (Gul, 1995) overestimated less and the position of the maximum is at the good energy.

In Fig. 2b we show the earlier ALICE-IPPE values (for reason of coherence with other figures), the new calculations by EMPIRE-II that are in rather good agreement with the experiment showing only an 8% overestimation and a 1.5 MeV upward shift while the values taken from the TENDL-2009 library show an excitation curve slightly shifted in energy and with a maximum reaching 740 mb (28% higher).

New recommended values (see Table 2c) for this reaction are derived from a SPLINE fit to a data set consisting of the 3 experimental curves and the EMPIRE Ii and TENDL-2009 results, scaled down by, respectively, 8% and 28% (see Fig. 2c).

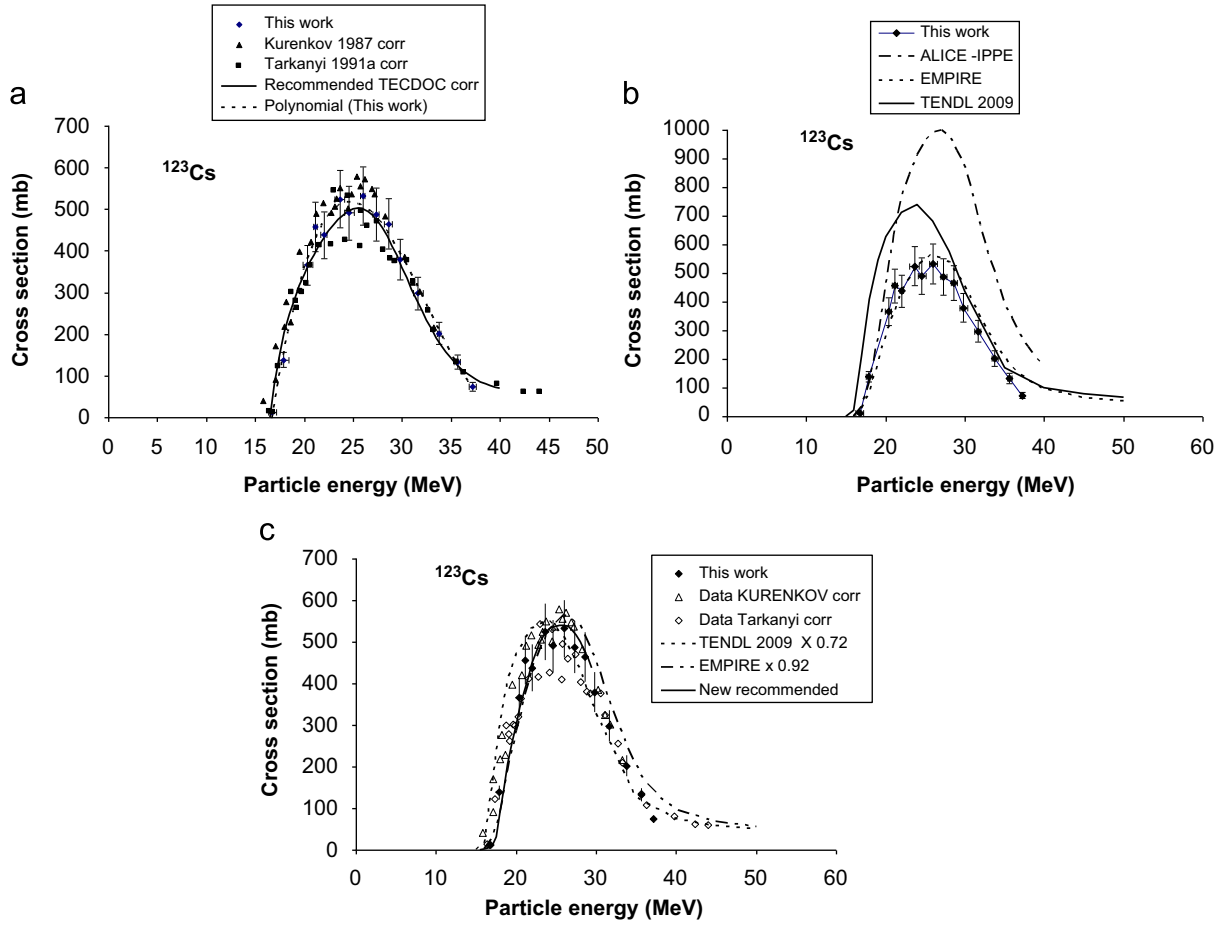

Fig. 2. (a) Excitation function for the ^{124}Xe(p,2n)^{123}Cs reaction and comparison with literature values. (b) Excitation function for the ^{124}Xe(p,2n)^{123}Cs reaction and comparison with theoretical codes. (c) Selected data sets for the ^{124}Xe(p,2n)^{123}Cs reaction and recommended excitation curve.

Table 2a
Cross sections (mb) for production of ^{123}Cs,^{123}Xe and ^{121}I through ^{124}Xe+ proton reactions.

E (MeV)	^{124}Xe(p,2n)^{123}Cs	^{124}Xe(p,2n+pn)^{123cum}Xe	^{124}Xe(p,pn)^{123}Xe		^{124}Xe(p,α)^{121}I
			polynomial fit	measurement	
9.1 ± 1.7					0.1 ± 0.02
12.4 ± 0.3					1.0 ± 0.2
14.0 ± 0.5					2.4 ± 0.4
15.5 ± 0.5		3.0 ± 0.4	3.0	3.0 ± 0.8	4.6 ± 0.7
16.7 ± 0.5	12.0 ± 1.6	83 ± 11	71.0	71 ± 18	5.8 ± 0.9
17.9 ± 0.4	139 ± 18	369 ± 48	217.0	220 ± 55	9.9 ± 1.5
20.3 ± 0.4	367 ± 48	645 ± 84	264.5	265 ± 66	12.6 ± 1.5
21.1 ± 0.3	457 ± 59	746 ± 97	275.7	318 ± 79	12.9 ± 1.6
22.0 ± 0.2	438 ± 57	743 ± 97	286.2	273 ± 68	12.4 ± 1.5
23.6 ± 0.6	525 ± 68	784 ± 102	299.1	272 ± 68	11.0 ± 1.3
24.6 ± 0.5	491 ± 64	807 ± 105	303.2	287 ± 72	9.4 ± 1.4
26.0 ± 0.5	532 ± 69	841 ± 109	304.5	330 ± 82	8.8 ± 1.3
27.3 ± 0.4	488 ± 63	823 ± 107	300.7	340 ± 85	6.0 ± 0.9
28.6 ± 0.4	465 ± 61	762 ± 99	292.5	320 ± 80	5.2 ± 0.8
29.8 ± 0.5	380 ± 49	650 ± 85	280.7	255 ± 64	4.6 ± 0.7
31.6 ± 0.4	298 ± 39	554 ± 72	256.5	241 ± 60	3.9 ± 0.6
33.8 ± 0.4	203 ± 26	406 ± 53	217.4	194 ± 49	4.5 ± 0.7
35.6 ± 0.3	133 ± 17	300 ± 39	174.6	171 ± 43	3.7 ± 0.6
37.2 ± 0.2	74 ± 10	226 ± 29	132.9	153 ± 38	3.5 ± 0.5

4.1.2. ^{123}Xe cumulative

The evolution of the ^{123}Xe activity was followed through assessment of its independent 178 and 330 keV γ-lines. The 149 keV line cannot be used as it is contaminated with longer lived ^{122}Xe (see further). The results of the 4th or 5th measurements (at least decay for 6 half-lives of the parent ^{123}Cs after EOB) are considered to be fully representing the total cumulative production of ^{123}Xe (Table 2a). The new experimental cross-section values and a polynomial fit to these points are shown in Fig. 3a. Also recalculated cumulative cross sections for the measurements by Kurenkov et al. (1989) and

Table 2b
Cross sections (mb) for production of ^{122}Xe and ^{121m,120g,119}I through ^{124}Xe+ protons.

E (MeV)	^{124}Xe(p,p2n)^{122}Xe	^{124}Xe(p,αn)^{120g}I	^{124}Xe(p,αn)^{120m}I	^{124}Xe(p,α2n)^{119}I
20.3 ± 0.4		2.0 ± 0.2		
21.1 ± 0.3		2.1 ± 0.3		
22.0 ± 0.2		4.6 ± 0.6		
23.6 ± 0.6		10.6 ± 1.3	1.2 ± 0.1	
24.6 ± 0.5		13.1 ± 1.6	1.9 ± 0.2	
26.0 ± 0.5		14.8 ± 1.8	2.8 ± 0.3	
27.3 ± 0.4	76 ± 10	18.1 ± 2.2	3.9 ± 0.5	
28.6 ± 0.4	86 ± 11	19.0 ± 2.3	4.4 ± 0.5	
29.8 ± 0.5	245 ± 32	21.3 ± 2.6	5.9 ± 0.7	4.3 ± 0.6
31.6 ± 0.4	298 ± 39	20.4 ± 2.4	5.8 ± 0.7	2.7 ± 0.4
33.8 ± 0.4	353 ± 46	18.3 ± 2.2	5.3 ± 0.6	8.3 ± 1.2
35.6 ± 0.3	383 ± 50	14.7 ± 1.8	4.1 ± 0.5	14.6 ± 2.2
37.2 ± 0.2	402 ± 52	10.5 ± 1.3	2.6 ± 0.3	19.6 ± 2.9

Table 2c
New recommended cross-section values (mb) for ^{124}Xe(p,2n)^{123}Cs and ^{124}Xe(p,2n+pn)^{123cum}Xe.

E (MeV)	^{123}Cs (mb)	^{123cum}Xe (mb)	*E* (MeV)	^{123}Cs (mb)	^{123cum}Xe (mb)
14.00		0.28	30.00	413.58	679.80
15.00		1.92	30.50	390.30	647.04
15.50	0.41	5.43	31.00	365.94	613.12
16.00	2.77	23.42	31.50	340.67	578.52
16.50	3.90	64.27	32.00	315.21	543.63
17.00	7.77	132.10	32.50	289.83	508.80
17.50	31.71	222.12	33.00	264.64	474.39
18.00	86.76	316.64	33.50	240.68	440.74
18.50	149.04	399.78	34.00	219.19	408.18
19.00	206.36	473.02	34.50	200.02	377.02
19.50	256.18	540.74	35.00	181.99	347.47
20.00	300.78	602.37	35.50	165.24	319.78
20.50	341.50	657.44	36.00	150.42	294.19
21.00	379.82	705.98	36.50	138.48	270.86
21.50	415.40	748.72	37.00	128.18	249.91
22.00	447.29	786.44	37.50	118.93	231.42
22.50	475.22	804.16	38.00	110.56	215.31
23.00	498.35	818.26	38.50	102.86	201.36
23.50	516.38	829.32	39.00	95.68	189.33
24.00	528.29	837.93	39.50	89.14	178.99
24.50	534.67	844.47	40.00	83.40	170.13
25.00	537.71	848.46	40.50	78.59	162.51
25.50	539.45	849.19	41.00	74.33	156.04
26.00	539.81	845.95	41.50	70.47	150.62
26.50	537.02	838.31	42.00	67.15	146.15
27.00	529.52	826.27	42.50	64.47	142.55
27.50	517.22	810.06	43.00	62.55	139.71
28.00	500.90	790.01	43.50	61.42	137.55
28.50	481.44	766.50	44.00	60.86	135.96
29.00	459.54	739.98	44.50	60.64	134.87
29.50	436.56	710.92	45.00	60.56	134.17

Tarkanyi et al. (1991a) are given, obtained by summing the uncorrected data for ^{123}Cs production and the cross sections for the direct (p,pn) reaction as published in the original articles. Although it was the cumulative cross section that was measured in these works, the values were not reported and can only be reconstructed through this approximation. The correspondence is rather good although the Tarkanyi values are clearly lower by about 15% and displaced to higher energy.

The theoretical values obtained with the ALICE-IPPE, EMPIRE II and TALYS codes (as sum of the ^{124}Xe(p,2n) and ^{124}Xe(p,pn) cross sections) overestimate the experimental values by 20–50% and energy shifts of maximums are noted for all of them (Fig. 3a). A normalized curve derived from the TENDL-2009 results (factor 0.80) together with our new results and the Kurenkov et al. (1989) data are used for deriving a new set of recommended values indicated in Table 2c and in Fig. 3b.

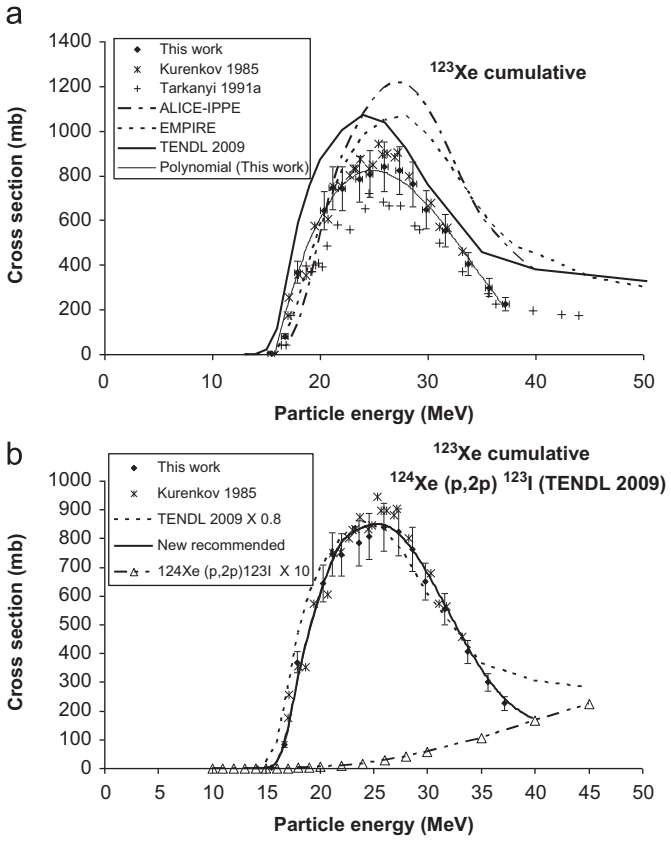

Fig. 3. (a) Excitation function for the ^{124}Xe(p,pn+2n)^{cum123}Xe reaction and comparison with theoretical codes and literature values. (b) Selected data sets for the ^{124}Xe(p,pn+2n)^{cum123}Xe reaction and recommended excitation curve.

4.1.3. *^{123}Xe direct*

In Fig. 4 the excitation function for the direct (p,pn) reaction is shown as derived by subtraction of our above discussed measurements. Both the data obtained by a subtraction for each of the energy points available in our measurements for ^{123}Cs and ^{123cum}Xe as the smoothed data obtained from the polynomial fits to the 2 data sets are shown and are in good correspondence. The uncertainties are high, as we have to add the uncertainties from both measured excitation functions.

The corrected values for this excitation function derived from Kurenkov et al. (1989) and Tarkanyi et al. (1991a) measurements (Figs. 2a and 3a) are also represented. As can be expected, these data are much closer to each other then what was published in the

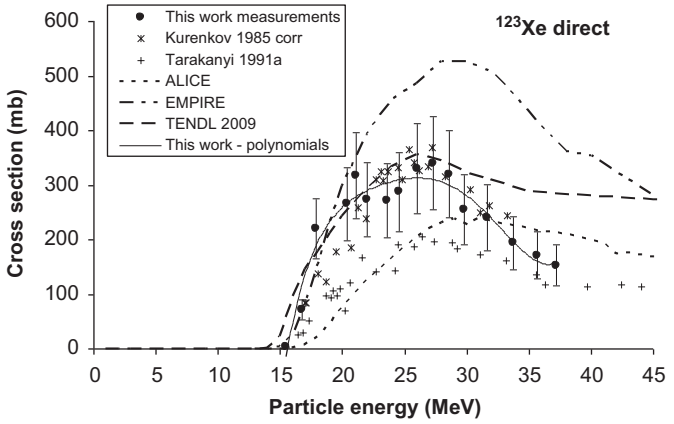

Fig. 4. Excitation function for the ^{124}X(p,pn) ^{123}Xe reaction and comparison with theoretical codes and literature values.

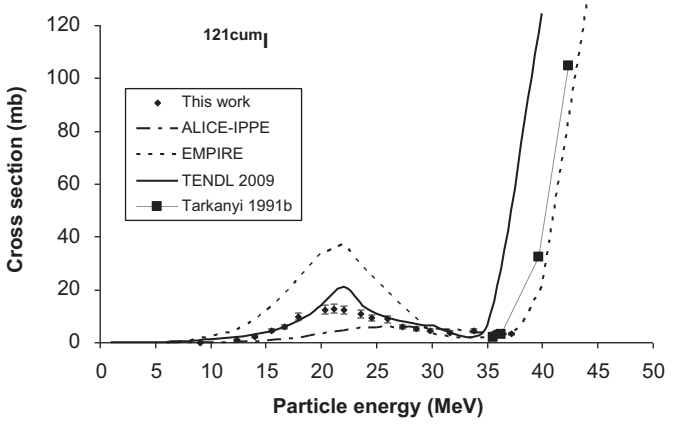

Fig. 5. Excitation function for the ^{124}X(p,α) ^{121}I reaction and comparison with theoretical codes and literature value.

TECDOC 1211 (IAEA, 2001) due to the lowering of the values for the ^{123}Cs cross section (outdated abundance for 596 keV line).

The results for the theoretical codes are rather disparate too. The ALICE-IPPE results underestimate essentially the measured values at low energies. The TENDL-2009 evaluation describes the data quite well at energies below the maximum, but shows the same tailing as ALICE-IPPE. The EMPIRE II results are overestimating by nearly 80% and are shifted to higher energies at the maximum like the ALICE-IPPE values.

The available experimental and calculated data do not allow yet proposing a recommended value although it could be obtained by the subtraction of the two sets proposed in the previous paragraphs.

4.1.4. *^{123}I direct by (p,2p)*

As was explained in previous paragraphs our experiments did not allow to determine reliable data for the direct production of ^{123}I because we did not wait long enough for total decay of ^{123}Xe in the cells and a part of the possible total ^{123}I activity was lost when recovering the enriched gas. It is also proven earlier that the cross sections for the direct production through the ^{124}Xe(p,2p) reaction are very low in the energy region studies as can be seen in Fig. 3b where the results of the latest TENDL calculation (multiplied by a factor of 10) are shown.

4.2. *Production of ^{121}I*

In the experimental (and production) conditions formation of very short lived ^{121}Cs through a (p,4n) reaction ($Q=-38$ MeV) and ^{121}Xe (38.8 min) through (p,p3n) ($Q=-29$ MeV) are impossible or extremely low (practical threshold of 1 mb at 38 MeV (Tarkanyi et al., 1991b). So only the direct production through a (p,α) reaction with a theoretical threshold of +3.8 MeV has to be considered here. The equivalent reaction with separate nucleons in the exit channel has a Q-value of -24.8 MeV and will only contribute significantly above 30 MeV.

The excitation curve for ^{121}I production (Fig. 5) shows a practical threshold at 9.5 MeV rising to a maximum of 13 mb at 21 MeV. The cross section is leveling off around 32 MeV but the expected rise due to the onset of the reactions with separate nucleons in the exit channel is not observed. Few points obtained by Tarkanyi et al. (1991b) at energies above 35 MeV are showing the expected behavior (see Fig. 5) and seem to be a good continuation of the present data.

The agreement with the theoretical results is not satisfying. While both the TALYS and EMPIRE II codes predict a shape and position of the maximum that can be considered compatible with the experiment their maximal values are double to triple. The ALICE-IPPE code on the contrary, on which up to now predictions for ^{121}I–^{121}Te contaminations in production runs were based, gives too low values and a large shift to higher energies. These discrepant results show that the (p,α) reaction is not well modeled with default parameters of the statistical codes and some adjustment of parameters could be recommended.

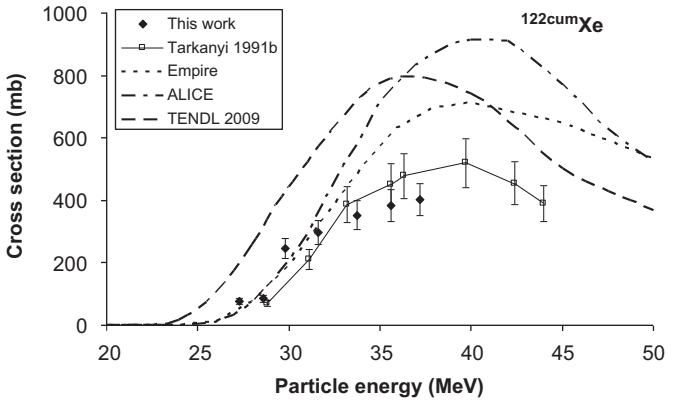

Fig. 6. Excitation function for the ^{124}X(p,p2n) ^{122}Xe reaction and comparison with theoretical codes and literature value.

4.3. *Production of ^{122}Xe*

The cumulative formation of this radioisotope with 20.1 h half-life (parents are the short lived ^{122m,g}Cs, respectively, with 4.2 m and 21 s half-lives, not detected) is measured by assessment of its independent γ-line at 350 keV. The strong line at 149 keV cannot be used as it is contaminated by a line of ^{123}Xe at the same energy!! Assessment through measurement of the short lived daughter ^{122}I ($T_{1/2}=3.6$ m) did not give good results.

The practical threshold of 24 MeV indicates that essentially the direct production by the (p,p2n) reaction ($Q=-18.44$ MeV) takes place (Fig. 6). The excitation functions rises sharply and reaches more than 400 mb at the highest energy studied (see Table 2b). No indication exists that at higher energy contribution through the (p,3n) reaction with $Q=-26.4$ MeV occurs. A comparison with the experimental results in Tarkanyi et al. (1991b) (EXFOR A0487) shows a good agreement in shape while they found a maximum of 520 mb at 40 MeV.

The 3 used codes give nearly analogous results with slight energy shifts for the maximum position but higher maximal values varying between 700 and 750 mb. The ALICE-IPPE estimation of maximal value looks abundantly high.

This radionuclide is not a real contaminant in the finally produced ^{123}I solution as it is eliminated by the I–Xe separation.

4.4. Production of ^{120m,g}I

These two isomers are positron emitters with high end-point β^+ energy and an attractive half-life for studying biodistribution of ^{123}I labeled compounds. In our experimental circumstances only direct production through the (p,αn) reaction is possible ($Q=-7.07$ MeV).

The possible parents, very short lived ^{120}Cs and ^{120}Xe ($T_{1/2}=40$ m) cannot be formed here as the Q-values of the reactions leading to their formation are, respectively, for (p,5n) $Q=-46.8$ MeV and for (p,p4n) $Q=-37.77$ MeV.

The high spin ($I^{\pi}=7^-$) ^{120m}I isomer ($T_{1/2}=53$ m) was measured by independent 601 and 614 keV γ-lines while ^{120g}I($T_{1/2}=1.35$ h), not formed by decay of meta state, is measured by the low abundance 641 keV line.

Both excitation functions (Fig. 7) show a practical threshold around 20 MeV and reach their maximum around 31 MeV. The isomer formation ratio is in the whole energy region studied in the favor of the ground state and decreases from a value of 8 at 23.6 MeV to about 4 at higher energies (see Table 2b). No other experimental data were found.

In Fig. 7 the results for the total formation of ^{120}I (ground +metastable state) calculated with 3 codes are shown. The TENDL-2009 results describe the experimental data quite well, although some overestimation at energies above the maximum is noted. The values obtained by EMPIRE II are too large by a factor of 4 while the ALICE-IPPE results are shifted in energy by more than 5 MeV and are underestimating the experiment slightly. The spread of theoretical curves around the experimental data is very similar to the results discussed above for the (p,α) reaction (Fig. 5), and could be again related to the default input parameters.

This radionuclide is not interesting for production of ^{120}I and has also no practical importance as contaminant production route as the ^{120}I would have decayed totally during the waiting time for ^{123}Xe–^{123}I in-growth while cross sections are also low.

4.5. Production of ^{119}I

The short-lived ($T_{1/2}=19$ m) ^{119}I was assessed through its 257 keV γ-line. The Q-values for formation of its parents ^{119}Cs–^{119}Xe are far beyond the energy range studied here (more than 50 MeV) so only the ^{124}Xe(p,α2n) reaction with $Q=-15.17$ MeV can occur. The practical threshold observed in Fig. 8 is much higher and the few data points available show a steeply increasing excitation function at higher energy. Numerical values are presented in Table 2b.

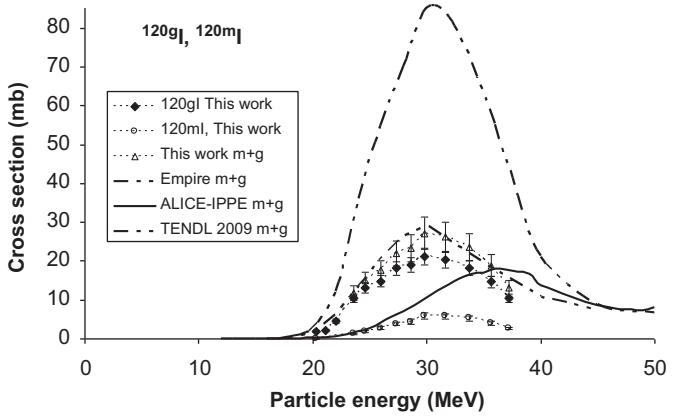

Fig. 7. Excitation function for the ^{124}X(p,αn) ^{120m,g}I reactions and comparison with theoretical codes.

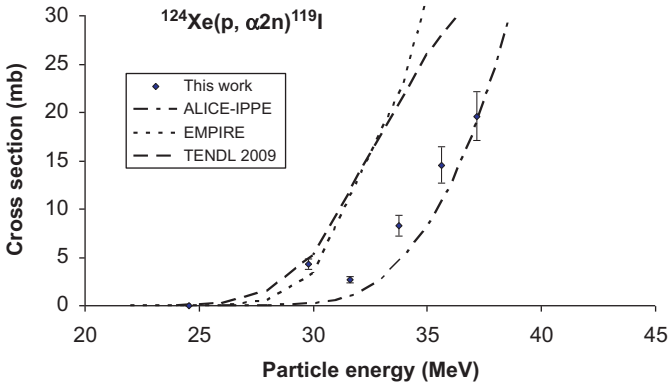

Fig. 8. Excitation function for the ^{124}X(p,α2n) ^{119}I reaction and comparison with theoretical codes.

Calculations for all used codes confirm the observed growth of excitation function and the obtained spread of calculations has the same reason as discussed above for the (p,α) and (p,αn) reactions.

Again this radioisotope is not a contaminant in practical ^{123}I production as at one hand saturation will be reached in the long irradiations and on the other hand it will decay out totally during the in-growth time. The ^{119}Te decay product (with half-life comparable to ^{123}I) will be removed during the chemical separation–purification step (see also next paragraph).

4.6. Thick target yields and contamination with ^{121}Te

As stated earlier an unavoidable contaminant in the final ^{123}I solution is the long lived ^{121g}Te with 16.8 d half-life.

Direct formation of ^{121g}Te, or the isomeric state ^{121m}Te (154 d), through the ^{124}Xe(p,3pn) reaction is not of importance because of the needed chemical separation between radio-iodine and radioactive or stable nuclides of any other element at the end of the ^{123}Xe-^{123}I in-growth period.

Hence the only contamination finds its origin in the decay of ^{121}I still present at the moment of this separation (ST).

The measurement of residual ^{121}Te, after precipitation and total decay of the ^{121}I, should hence be a direct means to estimate this contamination in the given irradiation and waiting circumstances. Unfortunately, the chemical procedure described above gave erratic results and the amount of ^{121}Te found is not in good agreement with the values obtained from the ^{121}I cross sections.

In order to estimate and possibly to identify the parameters allowing to minimize the ^{121g}Te contamination we developed a calculation sheet allowing to predict, on basis of the experimental excitation curve, the ^{121}I activity present at different cooling times (or separation times ST) after EOB in function of energy degradation in the target and of irradiation times (up to 22 h is used by MDS Nordion in Vancouver, more than 1 half-life of ^{123}I, full saturation of ^{121}I).

The evolution of the contaminating activity of both ^{121}I (decreasing in time) and ^{121}Te (increasing in time) can then further be followed in function of the time of use of the ^{123}I solution after the chemical separation (AST) (all ^{121}Te present at St is removed by the chemical procedure). By defining maximal admissible contaminations levels for late use of the ^{123}I solution, limits on target thickness or optimal irradiation and in-growth times are defined.

The available ^{123}I activity, and hence the contamination level, is obviously also dependent on all the irradiation and cooling parameters. As explained in the introduction, the optimal ^{123}Xe–^{123}I in-growth time for long irradiations is in the order of 2–3 h as the

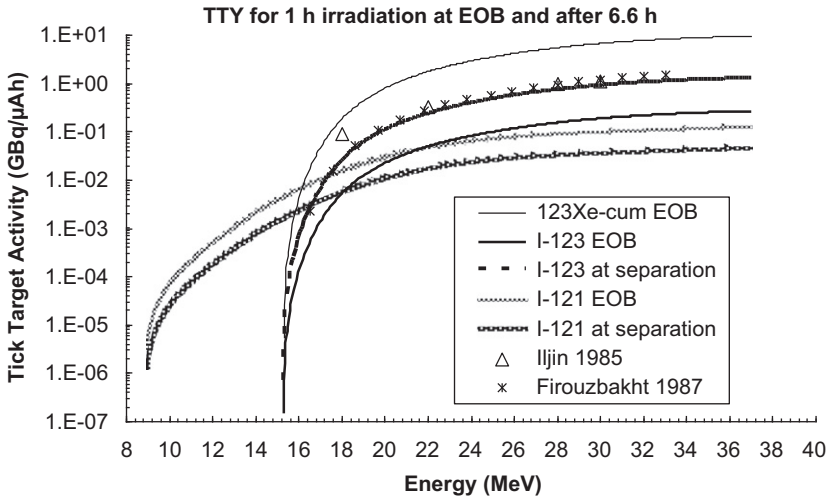

Fig. 9. Thick target yields at EOB and at EOB+ 6.6 h.

target contains at EOB already large amounts of ^{123}I formed during the irradiation.

For short irradiations (for instance 1 h) the optimal in-growth or separation time is 6.6 h, resulting in large increase of ^{123}I activity. The thick target yields at EOB, calculated for ^{123}Xe and ^{123}I from the recommended data for ^{123cum}Xe production given in Table 2c and for ^{121}I from the data in Table 2a are represented in Fig. 9 in function of the incident proton energy. Also the activities of ^{123}I and ^{121}I at EOB+ 6.6 h are indicated. As the experimental values for ^{123}I published by Firouzbakht et al. (1987) and Iljin et al. (1987) were obtained in comparable irradiation and waiting conditions, a comparison with our results can be made. Both early literature values agree well and are about 25% higher than our data.

Values for a more realistic 20 h irradiation time and for different separation times ST are represented in Fig. 10 for, respectively, 30 and 35 MeV incident energy and a target thickness resulting in an energy degradation of 12 MeV. Nearly no difference in maximal ^{123}I activity is observed (reached after 2 h in-growth) but the ^{121}I contamination level decreases strongly with longer ST and with higher incident energy.

In Fig. 11a,b influence of target thickness (expressed through energy degradation) and irradiation time on ^{123}I activity and ^{121}I contamination level in function of separation time ST is represented.

Also Table 3 gives some numerical examples of the different activity and contamination levels in function of the production parameters. It can be seen that while reducing the target thickness to obtain an exit energy of 28 MeV instead of 24 MeV has a minor incidence on the contamination level (reduction of 10%), it nearly halves the ^{123}I batch yield. Increasing the in-growth time by 2 h on the contrary (longer than optimal in-growth, additional decay of ^{121}I) results in 30% lower contamination level and only 10% reduction in ^{123}I. In Fig. 12 finally we represent the evolution of the ^{121}Te/^{123}I contamination level as function of the time of use after separation for different ^{121}I/^{123}I ratios at ST. An allowed 5×10^{-4} level at AST = 52 h corresponds hence to a contamination of 1% ^{121}I at separation.

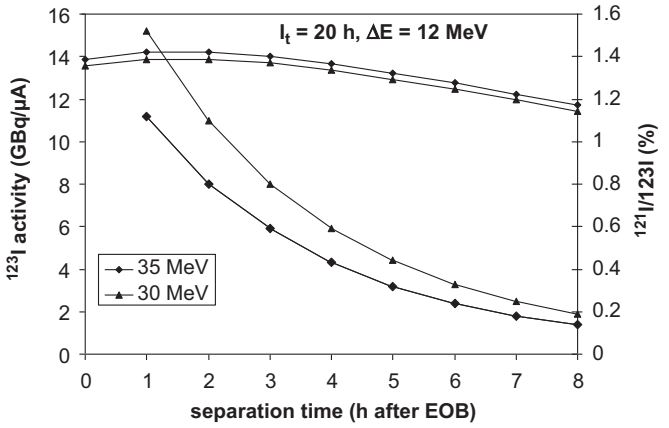

Fig. 10. ^{123}I activity and ^{121}I contamination levels for I_t = 20 h, ΔE = 12 MeV in function of separation time ST.

5. Conclusions

In a set of experiments with customized gas cells filled with highly enriched ^{124}Xe and irradiated with protons at 17 different incident energies between 9 and 38 MeV, the cross sections were measured for the 3 main radionuclides relevant to nca production of ^{123}I: the precursors ^{123}Cs, ^{123cum}Xe and the unavoidable contaminant ^{121}I.

Critical evaluation and comparison with the 2 available earlier literature data sets (Tarkanyi et al., 1991a; Kurenkov et al., 1989) and results from several theoretical codes allows to propose recommended values for the excitation functions of the ^{124}Xe(p,2n)^{123}Cs reaction and the ^{124}Xe(p,2n+pn)^{123cum}Xe route. The cross-section data for the direct production of ^{123}Xe through the (p,pn) reaction, derived from a difference between the 2 earlier mentioned pathways, are still scattered.

The first measurement of the ^{124}Xe(p,α)^{121}I excitation function over a wide energy region is strongly different (shift to lower energy and higher maximum) from the earlier (and only) calculated data by ALICE-IPPE. The new theoretical results by EMPIRE and TALYS predict even higher maximal values for this reaction.

On the basis of fits to the new data, thick target yield curves were calculated for ^{123cum}Xe and ^{121}I. A worksheet was developed to predict yields of ^{123}I (from ^{123}Xe decay) and contamination levels for ^{121}I and its decay product ^{121}Te in function of irradiation parameters, cooling/separation time and time of use of the ^{123}I solution after separation. It is shown that longer irradiation times and increase in cooling time before separation drastically reduces the contamination level while reduction of target thickness also improves contamination level but at the expense of decrease of overall ^{123}I batch yield. Higher incident energy, without increase of

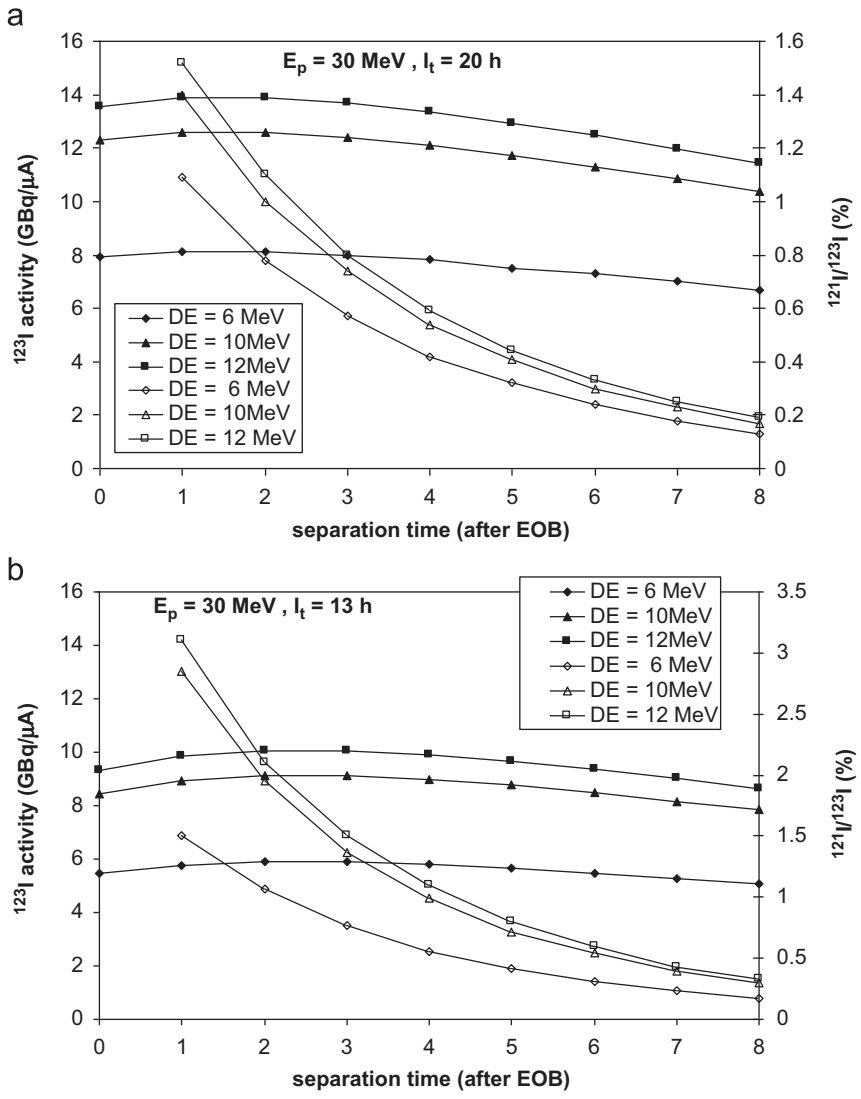

Fig. 11. (a,b) ^{123}I activity and ^{121}I contamination levels for I_t=20 h and I_t=13 h, E_{in}=30 MeV in function of target thickness and of separation time ST.

Table 3
Activities and contamination levels for different target thickness, irradiation time (I_t), separation time (ST), time of use after separation (AST).

$E_{in}-E_{out}$	Irradiation time I_t (h)	Time (h)		Activity (GBq/μA)			Contamination level (%)	
				^{123}I	^{121}I	^{121}Te	^{121}I/^{123}I	^{121}Te/^{123}I
35 – 28	13	EOB		5.00	9.73E – 02	5.49E – 04	1.95E+00	1.10E – 02
		ST	3	5.39	3.65E – 02	8.65E – 04	6.78E – 01	1.61E – 02
		AST	13	2.72	5.20E – 04	1.20E – 04	1.91E – 02	4.39E – 03
		AST	26	1.38	7.42E – 06	1.20E – 04	5.40E – 04	8.70E – 03
		AST	39	0.69	1.06E – 07	1.20E – 04	1.52E – 05	1.72E – 02
		AST	52	0.35	1.51E – 09	1.20E – 04	4.30E – 07	3.41E – 02
	13	EOB		5.00	9.73E – 02	5.49E – 04	1.95E+00	1.10E – 02
		ST	5	5.18	1.90E – 02	9.54E – 04	3.67E – 01	1.84E – 02
		AST	13	2.62	2.71E – 04	7.99E – 05	1.03E – 02	3.06E – 03
		AST	26	1.32	3.86E – 06	7.99E – 05	2.92E – 04	6.05E – 03
		AST	39	0.67	5.50E – 08	7.99E – 05	8.24E – 06	1.20E – 02
		AST	52	0.34	7.84E – 10	7.99E – 05	2.33E – 07	2.37E – 02
	13	EOB		5.00	9.73E – 02	5.49E – 04	1.95E+00	1.10E – 02
		ST	7	4.83	9.87E – 03	9.99E – 04	2.04E – 01	2.07E – 02
		AST	13	2.44	1.41E – 04	4.63E – 05	5.77E – 03	1.90E – 03
		AST	26	1.23	2.01E – 06	4.63E – 05	1.63E – 04	3.75E – 03
		AST	39	0.62	2.86E – 08	4.63E – 05	4.59E – 06	7.43E – 03
		AST	52	0.31	4.08E – 10	4.63E – 05	1.30E – 07	1.47E – 02
35 – 24	13	EOB		8.70	1.88E – 01	1.06E – 03	2.16E+00	1.22E – 02
		ST	3	9.37	7.03E – 02	1.67E – 03	7.51E – 01	1.78E – 02
		AST	26	2.39	1.43E – 05	2.30E – 04	5.98E – 04	9.63E – 03
		AST	52	0.61	2.91E – 09	2.30E – 04	4.76E – 07	3.77E – 02

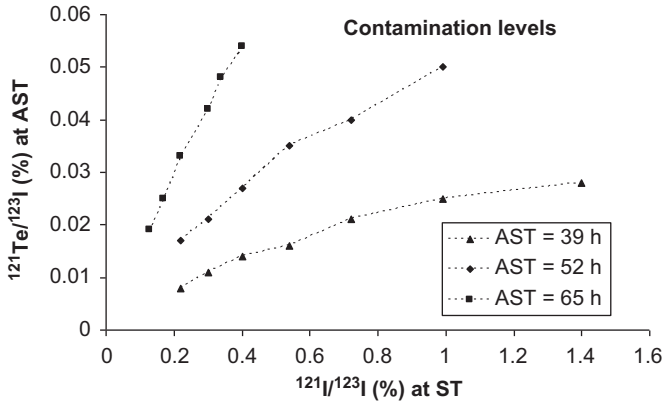

Fig. 12. Contamination levels for ^{121}Te at different AST in function of ^{121}I levels at ST.

target thickness has a negligible influence on both yield and contamination.

We should not forget that all these results are only valid for highly enriched ^{124}Xe targets. Presence of small amounts of ^{126}Xe (with same natural abundance as ^{124}Xe) will lead to unavoidable contamination with long lived ^{125}I.

The excitation curves for some minor, co-produced I and Xe radionuclides, are also measured.

The agreement between the results of the 3 theoretical codes used and the experimental data is in general not satisfying although in the case of ^{123}Cs and ^{123cum}Xe the predicted shape corresponds well enough so that normalized values could be used for inclusion in a combined data set for calculation of recommended values.

References

Andersen, H.H., Ziegler, J.F., 1977. Hydrogen—stopping powers and ranges in all elements. Volume 3 of Stopping and ranges of ions in matter. Pergamon Press, ISBN: 0-08-021605-6.

Belgya, T., Bersillon, O., Capote, R., Fukahori, T., Zhigang, G., Goriely, S., Herman, M., Ignatyuk, A.V., Kailas, S., Koning, A., Oblozhinsky, P., Plujko, V., Young, P., 2006. Handbook for Calculations of Nuclear Reaction Data, RIPL-2, IAEA-TECDOC1506, IAEA Vienna, Available from ⟨http://www-nds.iaea.or.at/RIPL-2/⟩.

Blann, M., 1996. New pre compound decay model (code ALICE-HMS). Phys. Rev. C 54, 1341–1349.

Browne, E., Firestone, R.B., 1986. In: Shirley, V.S. (Ed.), Table of Radioactive Isotopes. Wiley, New York.

Coenen, H.H., Mertens, J., Maziere, B., 2006. Radioiodination Reactions for Pharmaceuticals. Springer Verlag, Dordrecht.

Dityuk, A.I., Konobeyev, A.Yu., Lunev, V.P., Shubin, Yu.N., 1998. New advanced version of computer code ALICE-IPPE. Report INDC(CCP)-410, International Atomic Energy Agency, Vienna.

Firouzbakht, L.M., Teng, R.R., Schlyer, D.J., Wolf, A.P., 1992. Production of high purity iodine-123 from xenon-124: cross sections and yields. Radiochim. Acta 56, p167–p171.

Firouzbakht, L.M., Teng, R.R., Schlyer, D.J., Wolf, A.P., 1987. Production of iodine-123 from enon-124 at energies between15 and 34 MeV. Radiochim. Acta 41, 1–4.

Gul, K., 1995. A computer code based on Hauser-Fesbach and Moldauer theory for nuclear reaction cross section calculations. Report INDC (PAK) -011, IAEA Vienna.

Herman, M., Capote, R., Carlson, B.V., Oblozinsky, P., Sin, M., Trkov, A., Wienke, H., Zerkin, V., 2007. EMPIRE: Nuclear reaction model code system for data evaluation. Nucl. Data Sheets 108, 2655–2715.

IAEA 2001. Final report of a coordinated research project "Charged-particle cross section database for medical radioisotope production :Diagnostic radioisotopes and monitor reactions Contributors: S.M. Qaim, F. Tarkanyi, P. Oblozinsky, K. Gul, A. Hermanne, M.G. Mustafa, F.M. Nortier, B. Scholten, Y. Shubin, S. Takacs, Y. Zhuang, IAEA-TECDOC-1211, Vienna 2001. Available online at ⟨http://www-nds.iaea.org/medical/⟩.

Iljin, L.A., Germakov, I.A., Godov, V.I., Rostin, A.S., Zabrodin, B.V., Motornij, A.V., Shustrov, B.A., 1987. On the possibility of production of 13I from ^{124}Xe at MGC20 compact cyclotron. Current Questions in Medical Radiation Physics (Collection of Scientific Works, Leningrad), p 97.

ISO, 1993. Guide to the expression of uncertainty in measurement, 1995. International Organization for Standardization, Geneva, ISBN: 92-67-10188-9.

Kinsey, 1997. NuDat 2.5 database. Data source: National Nuclear Data Center, Brookhaven National Laboratory, based on ENSDF and the Nuclear Wallet Cards, available from ⟨http://www.nndc.bnl.gov/nudat2/⟩.

Koning, A.J., Rochman, D., TENDL-2009: TALYS-based Evaluated Nuclear Data Library. Nuclear Research and Consultancy Group (NRG) Petten, The Netherlands. ⟨http://www.talys.eu/tendl-2009beta/⟩.

Konyahin, N.A., Mironov, V.N., Krasnov, N.N., Dmitriev, P.P., Lapin, V.P., Paparin, M.V., 1989. Yield of ^{123}I from proton bombardment of ^{124}Xe over the energy range 16–21.5 MeV. At. Energ. 67, 129.

Kurenkov, N.V., Malinin, A.B., SEbyakin, A.A., Venikov, N.I., 1989. Excitaion functions of proton induced nuclear reactions on Xe-124: production of I-123. J. Radioanal. Nucl. Chem. Lett. 135, 39.

Oberdorfer, F., Meissner, M., Tiede, A., Schweickert, H., 2009. Advanced high current target technology for large scale ^{123}I and ^{18}F production. ZAG Zyklotron AG, Eggenstein-Leopoldshafen, Germany. Final report of CRP on high current targets, IAEA, Vienna 2009.

Sonck, M., van Hoyweghen, J., Hermanne, A., 1996. Determination of external beam energy of a variable energy multiparticle cyclotron. Appl. Radiat. Isot. 47, 445–449.

Takacs, S., Tarkanyi, F., Sonck, M., Hermanne, A., 2002. New cross-sections and intercomparison of proton monitors reactions on Ti, Ni and Cu. Nucl. Instr. Methods B 188, 106–111.

Tarkanyi, F., Kovacs, Z., Qaim, S.M., Stocklin, G., 1989. Differential production yields of ^{123}I in proton and deuteron induced reactions on natural xenon. Radiochim. Acta 47, 25.

Tarkanyi, F., Qaim, S.M., Stocklin, G., Sajjad, M., Lambrecht, R.M., Schweikert, H., 1991a. Excitation functions of (p,2n) and (p,pn)reactions and differential and integral yields of ^{123}I in proton induced reactions on highly enriched ^{124}Xe. Appl. Radiat. Isot. 42, 221.

Tarkanyi, F., Qaim, S.M., Stocklin, G., Sajjad, M., Lambrecht, R.M., 1991b. Nuclear cross sections relevant to the production of the ^{122}Xe-^{122}I generator system using highly enriched ^{124}Xe and a medium-sized Cyclotron. Appl. Radiat. Isot. 42, 229.

Tárkányi, F., Szelecsényi, F., Takács, S., 1991c. Determination of effective bombarding energies and fluxes using improved stacked-foil technique. Acta Radiol. Supplementum 376, 72.

Tarkanyi, F., Takacs, S., Heselius, S.J., Solin, O., Bergman, J., 1997. Static and dynamic effects in gas targets use for medical isotope production. Nucl. Instr. Methods Phys. Res. Sect. A 397, 119–127.

Tárkányi, F., Hermanne, A., Takács, S., Rebeles, R.A., Van den Winkel, P., Király, B., Ditrói, F., Ignatyuk, A.V., 2009. Cross section measurements of the ^{131}Xe(p,n) reaction for production of the therapeutic radionuclide ^{131}Cs. Appl. Radiat. Isot. 67, 1751–1757.

Venikov, N.I., Novikov, V.I., Sebyakin, A.A., Formichev, D.I., Shabrov, V.A., Kurchatov, I.V., 1991. Production of high-purity ^{123}I on IAE Cyclotron. In: Matin, B., Ziegler, K., (Eds.), Proceedings of the 12th International Conference on Cyclotrons and their Applications, pp. 519–522.